

## NUMERICAL OPTIMAL POLLUTION CONTROL SUBJECT TO THE CONVECTION-DIFFUSION TRANSPORT EQUATIONS

YUJING YUAN AND DONG LIANG\*

**Abstract.** In this paper, we develop an optimal control approach of pollution and emission reduction subject to convection-diffusion transport equations. A linked simulation-optimization method has been proposed, based on solving the convection-diffusion transport equations and solving the optimization procedure. The governing equations of the convection-diffusion-reaction equations with pollution sources are discretized by the splitting improved upwind finite volume scheme while the constrained differential evolution (DE) algorithm is applied to solve the global optimization procedure. The advantage of the approach is the external linking of the numerical simulation and the optimization procedure, minimizing both the weighted deviation between simulated concentrations and the smallest allowable concentrations at observation sites and the emission reduction cost at the pollution sources at same time. Numerical tests first check the convergence of numerical methods. Numerical experiments then show the performance of the approach for solving the optimal control problems of pollution and cost of emission reduction. The developed optimal control approach is efficient and it can be applied to more complex problems in applications.

**Key words.** Optimal pollution control, convection-diffusion equation, emission reduction cost, improved-upwind FV method, splitting.

### 1. Introduction

There are noticeable achievements in the development of economy, but the environment is recently deteriorating. For controlling and improving serious pollution of environment, the emission reduction plays an important role in the practical pollutant governing and balanced development. The common problems encountered over the world are groundwater pollution and air pollution ([2, 4, 5, 10, 12]). Emission control is the essential method to improve and control pollution and to protect the environment.

However, it is difficult to design the discharge strategy until the sources are identified with respect to their locations and magnitudes. Over the years, some methodologies have been proposed for groundwater source identification, such as the non-linear least-squares method [1], the geo-statistical approach [2], the constrained robust least square approach [15]. Paper [10] considered simultaneous estimation of aquifer parameters and identification of unknown pollution sources. Paper [12] used the artificial neural network for considering simple and complex scenarios, where the results were promising even with large measurement errors. But, during the procedure of minimizing the pollution, there is of great interest and difficulty to consider the cost affection of the controlling and reducing pollution emission in the real applications. Thus, it is an important task to study and develop the optimal control approach to the global optimization of pollution by considering the reduction cost in the environmental control and management.

In this paper, we propose a new optimal pollution control by minimizing the difference between the simulated concentration and the best environment allowing

---

Received by the editors September 20, 2016 and, in revised form, February 28, 2017.

2000 *Mathematics Subject Classification.* 65M10, 65M15, 65N10, 65N15.

\*Corresponding author. *E-mail:* dliang@mathstat.yorku.ca.

concentration at observation sites and the cost of the emission reduction at the pollution source points. A linked simulation-optimization model has been developed, based on the two-dimensional convection-diffusion transport equations and the differential evolution (DE) optimization algorithm. The advantage of the approach is the external linking of numerical simulation and the optimization procedure. Different from [10], our optimization objective function includes two terms. While the first term aims at minimizing the weighted deviation between the simulated concentration and the best environment allowing concentration at observation sites over time, the second term makes the cost of emission reduction as small as possible. The proposed optimal pollution control model is subject to the convection-diffusion transport equations and two other kind constraints of state and control. In the numerical scheme for solving convection-diffusion transport equations, we propose to use the operator splitting scheme combining with the improved-upwind finite volume method. The two-dimensional problems are split into two one-dimensional problems at each time step, and the second-order improved-upwind finite volume method avoids nonphysical oscillation and obtains the high accuracy. The constrained differential evolution (DE) optimization algorithm is considered to solve the optimization procedure, which provides the advantages of its global solution solving feature, simplicity, powerful search capability, compact structure and high convergence. Numerical tests firstly show the second-order accuracy of the improved-upwind FV method. We then give numerical experiments of the optimal control problems of pollution. For an example without considering the emission reduction cost, numerical results are given for the cases with different levels of perturbation to observation data and different locations of the source points and observation sites. Two other examples are finally considered for the cases involved emission reduction costs with different cost functions, where it also considers different observation locations and different flow velocities. Numerical results show that the emission reduction rates can be found for the optimal pollution control and the pollution control depends on the choice of protected zones and also depends on the velocity of flow. The developed optimal control approach is efficient and it can be applied to more complex pollution control problems in applications.

This paper is organized as follows. In Section 2, we present the governing equations of the two-dimensional convection-diffusion transport problems with the local point sources and then propose the optimal pollution control model. In Section 3, the numerical schemes and the optimization algorithm are given. In Section 4, numerical experiments are taken and analyzed.

## 2. Formulation of Optimal Control Problems

**2.1 The governing equations.** We consider the pollution problems with a polluted region  $\Omega \subset R^2$  and boundary  $\Gamma$ , where the pollutant is discharged through  $n_s$  outfalls (see Figure 1). The pollution of contaminant is governed by the two-dimensional convection diffusion reaction equations with point sources.

$$(1) \quad \frac{\partial c}{\partial t} + \vec{v} \cdot \nabla c - \frac{\partial}{\partial x} \left( D_x \frac{\partial c}{\partial x} \right) + \frac{\partial}{\partial y} \left( D_y \frac{\partial c}{\partial y} \right) + Rc = \sum_{l=1}^{n_s} q_l(t) \delta(x - x_{s_l}, y - y_{s_l})$$

$$(x, y) \in [0, L_x] \times [0, L_y], t \in (0, T),$$

$$(2) \quad c(x, y, 0) = c_0(x, y), \quad (x, y) \in [0, L_x] \times [0, L_y],$$

$$(3) \quad c(0, y, t) = 0, \frac{\partial c(L_x, y, t)}{\partial x} = 0, \quad y \in [0, L_y], t \in [0, T],$$

$$(4) \quad \frac{\partial c(x, 0, t)}{\partial y} = \frac{\partial c(x, L_y, t)}{\partial y} = 0, \quad x \in [0, L_x], t \in [0, T],$$

where  $c(x, y, t)$  is the dissolved concentration of pollutant, and  $c_0(x, y)$  is the initial concentration of pollutant.  $\vec{v} = (v_x, v_y)^T$  denotes the average velocity of flow;  $D_x$  and  $D_y$  are, respectively, the longitudinal and transversal dispersion coefficients,  $R$  is a reaction coefficient describing the self-purifying function. The right hand side term is the point source term that causes the pollution. Suppose that all the outfalls are located at the points  $S_l = (x_{s_l}, y_{s_l}), l = 1, 2, \dots, n_s$ , where  $(x_{s_l}, y_{s_l})$  is the location of source point. In Figure 1, taking  $n_s = 4$  gives an example of four point sources. Denote by  $q_l(t)$  the mass disposal fluxes of pollutant at the points  $s_l, l = 1, 2, \dots, n_s$ .

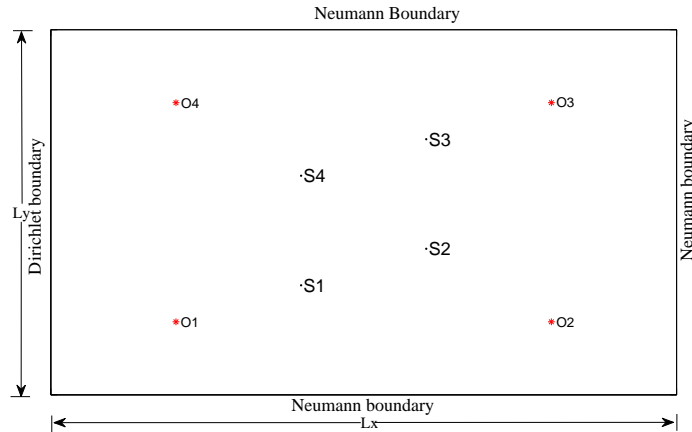


**Fig. 1.** Diagram of the domain with source points ( $S_i$ ) and observation sites ( $O_j$ ).

**2.2 The optimal control problem.** To achieve the optimal control of pollution and reduction cost, an embedding optimization model subject to the constraint of partial differential equations is proposed in this sub-section. The basic goal of the optimization model is to find the strength of emission and the rate of emission reduction for minimizing the combined objective function of the weighted differences of simulated concentration with optimal environment allowable concentration and the cost that needs to pay for reducing the discharges at the pollution sources.

The combined objective function is defined as

$$(5) \quad J(\vec{q}) = \sum_{s=1}^{n_r} \int_0^T \omega_s(t) [c_s(\vec{q}, t) - c_s^*(t)]^2 dt + \sum_{l=1}^{n_s} \int_0^T g_l(q_l) dt,$$

where  $\vec{q} = (q_1(t), q_2(t), \dots, q_{n_s}(t))^T$ .

Then, the optimal control problem can be proposed as

$$(6) \quad \min_{\vec{q}} J(\vec{q})$$

subject to:

$$(7) \quad \text{Eqns. (1) - (4),}$$

$$(8) \quad \vec{q}^{min} \leq \vec{q} \leq \vec{q}^{max},$$

$$(9) \quad \vec{c}^{min} \leq \vec{c} \leq \vec{c}^{max},$$

where  $\vec{c} = (c_1(t), c_2(t), \dots, c_{n_r}(t))^\tau$  is the simulated concentration vector at observation points, and  $\vec{c}^{min}$  and  $\vec{c}^{max}$  are the low and upper bounds of concentrations during the time period.  $\vec{q}^{min} = (q_1^{min}, q_2^{min}, \dots, q_{n_s}^{min})^\tau$  are the lowest pollution disposal fluxes and  $\vec{q}^{max} = (q_1^{max}, q_2^{max}, \dots, q_{n_s}^{max})^\tau$  are the upper bounds of the pollution disposal fluxes at the pollution sources.  $O_s, s = 1, 2, \dots, n_r$ , are observation points and  $n_r = 4$ , as shown in Figure 1.

Constraint (7) represents the externally linked simulation model that transforms the source mass disposal fluxes at various potential source locations into concentration  $\vec{c}$  in the pollution domain as a function of  $\vec{q}$ . The lower and upper bounds on the source disposal fluxes in Constraint (8) ensure that the practically acceptable discharges are considered. Because any production will induce pollution, when the quantity of disposal reach a certain threshold, the environment is contaminated, the lower bounds of discharge fluxes can refer to this threshold. Constraint (9) guarantees that once resulting concentrations are evaluated for an assumed set of source disposal fluxes, only those  $\vec{q}$  are acceptable, which result in the simulated concentration  $\vec{c}$  within some predefined lower and upper bounds. In the computation of the optimal control model presented here, all the lower bounds of the concentrations are taken as zero, or the values close to zero. On the other hand, if the quantity of pollutant exceeds a value, it will lead to important change in the ecosystem, the values are thought as the upper bounds of pollutant concentration.

In the objective function (5),  $c_s^*(t), s = 1, 2, \dots, n_r$ , denote the environmental allowable concentrations at observation points, they are the observed values and usually obtained from sampling with low pollution sources. In numerical experiments, we generally use the perturbed numerical results from low disposals at pollution sources to instead the observed values. In this paper, we use the environmental allowable concentrations obtained from the disposal fluxes  $\vec{q} = \vec{q}^{min}$ , and thus the first term of the objective function is to aim at minimizing the deviation between the concentrations and the concentrations from the smallest disposal fluxes.

The weights  $\omega_s(t)$  are defined as:

$$\omega_s(t) = \frac{1}{[c_s^*(t) + \eta]^2}, \quad s = 1, 2, \dots, n_r,$$

which are intended to normalize the terms of the objective function. It is preferable to add a constant to the observation concentration to prevent small difference at low concentration to dominate the objective function.  $\eta$  generally depends on the order of the concentration values. In the real life problem, it may be a fraction of the difference between largest and smallest concentration values.

On the other hand, the second term of the objective function (5) is to reflect the cost affection of emission reduction. In reality, we know that the cost will be less when the reduction rate is smaller, which means with relative larger disposal fluxes. For the cost function of the emission reduction, we consider the following two kinds of functions:

$$(10) \quad g_l(q_l) = a_l Q_l^2 + b_l Q_l,$$

$$(11) \quad g_l(q_l) = c_l (e^{d_l Q_l} - 1),$$

where  $a_l, b_l, c_l$  and  $d_l$  are parameters,  $l = 1, 2, \dots, n_s$ , and  $Q_l$  is the emission reduction rate at source point  $S_l$ , which is define as

$$(12) \quad Q_l = \frac{q_l^{max} - q_l(t)}{q_l^{max}}.$$

The emission reduction cost depends not only on the kind of pollutants but also on the sort and scale of pollutants, where the different coefficients of the cost functions will distinguish the differences. Our goal is to minimize the the objective function (5) of the joint affection of pollution and cost of emission reduction.

**3. Numerical scheme and optimization algorithm**

**3.1 Numerical scheme for PDEs.** Before giving the numerical schemes, we first concentrate on the two-dimensional Delta function. As we know, it has the form as

$$(13) \quad \delta(x, y) = \begin{cases} +\infty, & x = 0, y = 0, \\ 0, & otherwise, \end{cases}$$

satisfying the constraint condition

$$(14) \quad \int_{-\infty}^{+\infty} \int_{-\infty}^{+\infty} \delta(x, y) dx dy = 1.$$

In computation, we take the Gaussian function to approximate it as

$$(15) \quad \varphi_l(x, y) = \begin{cases} \frac{1}{4\pi\epsilon} \exp(-\frac{(x-x_{s_l})^2}{4\epsilon} - \frac{(y-y_{s_l})^2}{4\epsilon}), & |x - x_{s_l}| \leq 2\sqrt{2\epsilon}, |y - y_{s_l}| \leq 2\sqrt{2\epsilon}, \\ 0, & otherwise, \end{cases}$$

As  $\epsilon \rightarrow 0$ , it converges to the Delta function.

To get the discretization form of problem (1) - (4), we divide  $\Omega$  equally. Let  $0 = x_0 < x_1 < \dots < x_{n_x} = L_x$  and  $0 = y_0 < y_1 < \dots < y_{n_y} = L_y$  be the partitions of  $[0, L_x] \times [0, L_y]$  in  $x$  and  $y$  directions, respectively. The space step sizes are defined by  $h_x = L_x/n_x$  and  $h_y = L_y/n_y$ , and the grid points are  $(x_i, y_j) = (ih_x, jh_y)$ . Likewise, we discretize the time domain similarly by placing a grid on the temporal axis with time step size  $\Delta t = T/n_t$ , where  $n_t$  is the number of total temporal steps.

Notationally, we let  $C_{i,j}^k$  approximate  $c(x_i, y_j, t_k)$ . Let  $q_l^k$  means  $q_l(t)$  at  $t = k\Delta t$ . Here we suppose the pollutant source points are all in grids points,  $(x_{s_l}, y_{s_l}) = (i_{s_l}h_x, j_{s_l}h_y)$ , where  $l = 1, 2, \dots, n_s$ , and  $i_{s_l}, j_{s_l}$  are the location index numbers of the  $l^{th}$  pollution point along the  $x$ -direction and the  $y$ -direction respectively.

We will apply the splitting technique to solve the two-dimensional governing equations, where the corresponding coefficient matrix of the algebraic system for each step is a tridiagonal matrix and the system can be easily solved with very low computational cost. On the other hand, in the pollution procedure, the diffusion coefficients are much smaller than transport velocity, which leads to a difficulty of solving the convection dominated problems. They often have nonphysical oscillations into numerical solutions by the standard finite difference methods or finite element methods while they have only first order accuracy in spacial step size by the standard upwind schemes (see, for example, [6, 16], etc). In order to obtain the accurate numerical solution, the modified upwind schemes improve the accuracy without introducing the nonphysical numerical oscillations ([4, 7, 8], etc).

In computation, we propose the splitting scheme combining with the modified upwind technique. Letting

$$D_x^* = \frac{D_x}{1 + \frac{h_x v_x}{2D_x}}, D_y^* = \frac{D_y}{1 + \frac{h_y v_y}{2D_y}},$$

the improved upwind finite volume scheme (IUFVS) for solving the convection diffusion equations is defined as

For  $n = 0, 1, \dots, n_t - 1$ , do the following steps:

**Step 1.** For  $j = 0, 1, 2, \dots, n_y$ ,

$$(16) \quad \begin{aligned} & \frac{C_{i,j}^{n+\frac{1}{2}} - C_{i,j}^n}{\Delta t} + v_x \frac{C_{i,j}^{n+\frac{1}{2}} - C_{i-1,j}^{n+\frac{1}{2}}}{h_x} - D_x^* \frac{C_{i+1,j}^{n+\frac{1}{2}} - 2C_{i,j}^{n+\frac{1}{2}} + C_{i-1,j}^{n+\frac{1}{2}}}{h_x^2} + RC_{i,j}^{n+\frac{1}{2}} \\ & = \sum_{l=1}^{n_s} q_l^{n+1} \varphi_l(ih_x, jh_y), \quad i = 1, 2, \dots, n_x. \end{aligned}$$

**Step 2.** For  $i = 1, 2, \dots, n_x$ ,

$$(17) \quad \frac{C_{i,j}^{n+1} - C_{i,j}^{n+\frac{1}{2}}}{\Delta t} + v_y \frac{C_{i,j}^{n+1} - C_{i,j-1}^{n+1}}{h_y} - D_y^* \frac{C_{i,j+1}^{n+1} - 2C_{i,j}^{n+1} + C_{i,j-1}^{n+1}}{h_y^2} = 0, \\ j = 0, 1, \dots, n_y.$$

The discrete boundary conditions are:

$$(18) \quad C_{0,j}^{n+\frac{1}{2}} = 0, j = 0, 1, \dots, n_y,$$

$$(19) \quad \frac{C_{n_x+1,j}^{n+\frac{1}{2}} - C_{n_x-1,j}^{n+\frac{1}{2}}}{2h_x} = 0, j = 0, 1, \dots, n_y,$$

$$(20) \quad \frac{C_{i,1}^{n+1} - C_{i,-1}^{n+1}}{2h_y} = 0, i = 1, 2, \dots, n_x,$$

$$(21) \quad \frac{C_{i,n_y+1}^{n+1} - C_{i,n_y-1}^{n+1}}{2h_y} = 0, i = 1, 2, \dots, n_x.$$

With boundary condition (19), scheme (16) can be rewritten as, for  $j = 0, 1, \dots, n_y$ ,

$$(22) \quad aC_{i-1,j}^{n+\frac{1}{2}} + bC_{i,j}^{n+\frac{1}{2}} + dC_{i+1,j}^{n+\frac{1}{2}} = C_{i,j}^n + \Delta t \sum_{l=1}^{n_s} q_l^{n+1} \varphi_l(ih_x, jh_y), i = 1, 2, \dots, n_x - 1,$$

$$(23) \quad (a + d)C_{n_x-1,j}^{n+\frac{1}{2}} + bC_{n_x,j}^{n+\frac{1}{2}} = C_{n_x,j}^n + \Delta t \sum_{l=1}^{n_s} q_l^{n+1} \varphi_l(n_x h_x, jh_y),$$

where

$$\begin{aligned} a &= -\frac{\Delta t}{h_x^2} D_x^* - \frac{\Delta t}{h_x} v_x, \\ b &= 1 + 2\frac{\Delta t}{h_x^2} D_x^* + \frac{\Delta t}{h_x} v_x + R\Delta t, \\ d &= -\frac{\Delta t}{h_x^2} D_x^*. \end{aligned}$$

With boundary condition (20) (21), scheme (17) can be rewritten as: for  $i = 1, 2, \dots, n_x$ ,

$$(24) \quad a' C_{i,j-1}^{n+1} + b' C_{i,j}^{n+1} + d' C_{i,j+1}^{n+1} = C_{i,j}^{n+\frac{1}{2}}, j = 1, 2, \dots, n_y - 1,$$

$$(25) \quad b' C_{i,0}^{n+1} + (a' + d') C_{i,1}^{n+1} = C_{i,0}^{n+\frac{1}{2}},$$

$$(26) \quad (a' + d') C_{i,n_y-1}^{n+1} + b' C_{i,n_y}^{n+1} = C_{i,n_y}^{n+\frac{1}{2}},$$

where

$$\begin{aligned} a' &= -\frac{\Delta t}{h_y^2} D_y^* - \frac{\Delta t}{h_y} v_y, \\ b' &= 1 + 2\frac{\Delta t}{h_y^2} D_y^* + \frac{\Delta t}{h_y} v_y, \\ d' &= -\frac{\Delta t}{h_y^2} D_y^*. \end{aligned}$$

System (22)-(23) and system (24)-(25) are tridiagonal systems. Solving the systems alternately, we will have the numerical solutions at time level  $t^k$  as

$$(27) \quad C^k = F(\vec{q}, C^{k-1}),$$

where  $C^k = (C_{i,j}^k)_{n_x \times n_y}$ ,  $k = 1, 2, \dots, n_t$ ;  $F(\vec{q}, C^{k-1})$  represents the externally linked simulation model that transforms the source mass disposal fluxes, into concentration  $C^k$ ,  $F$  is the solution operator of the discrete process.

In the discrete form, the discrete objective function can be described as:

$$(28) \quad J_h(\vec{q}) = \sum_{k=1}^{n_t} \sum_{s=1}^{n_r} \Delta t \omega_s^k (C_s^k - C_s^{*k})^2 + \sum_{k=1}^{n_t} \sum_{l=1}^{n_s} \Delta t g_l(q_l^k).$$

We aim at finding  $\vec{q} = (q_1, q_2, \dots, q_{n_s})$  such that

$$(29) \quad \min_{\vec{q}} J_h(\vec{q})$$

subject to:

$$(30) \quad C^k = F(\vec{q}, C^{k-1}),$$

$$(31) \quad C_s^{k,min} \leq C_s^k \leq C_s^{k,max}, \quad s = 1, 2, \dots, n_r,$$

$$(32) \quad q_l^{min} \leq q_l \leq q_l^{max}, \quad l = 1, 2, \dots, n_s,$$

where  $C_s^k = C_{i_s, j_s}^k$ ,  $s = 1, 2, \dots, n_r$ , are the simulated concentration at observation sites  $(x_{i_s}, y_{j_s})$ ,  $s = 1, 2, \dots, n_r$ , with the disposal rate  $\vec{q}$  at pollution points.  $C_s^{k,min}$  and  $C_s^{k,max}$  are the lower and upper bounds at the observation sites. The specified concentration  $C_s^{*k}$  is corresponding to the solution with the smallest disposal rate  $\vec{q} = \vec{q}^{min}$ .

**3.2 The optimization algorithm.** In the computation of the optimal control problems, we propose to apply the Differential Evolution (DE) algorithm to solve the optimal control problem of pollution and cost optimization. This algorithm does not need to compute the gradient of objective function, which was proposed in [13, 14] to solve optimization problems over continuous domains. Further development was done to solve the multi-objective problems [11]. The constrained DE algorithm was studied to tackle constrained optimization problems in [9, 17], etc. The DE algorithm is simple and straightforward to implement and has powerful search capability and high accurate characteristics with using only few number of control parameters.

We let  $D = [q_1^{min}, q_1^{max}] \times [q_2^{min}, q_2^{max}] \times \dots \times [q_{n_s}^{min}, q_{n_s}^{max}]$  and the restriction condition (31) rewritten as:

$$\begin{aligned} f_i^k(\vec{q}) &= C_s^k - C_s^{k,max} \leq 0, \quad s = 1, 2, \dots, n_r, k = 1, 2, \dots, n_t, \\ f_i^{nt+k}(\vec{q}) &= C_s^{k,min} - C_s^k \leq 0, \quad s = 1, 2, \dots, n_r, k = 1, 2, \dots, n_t. \end{aligned}$$

Define the function  $\phi(x)$ , called satisfaction degree function, to estimate the violation with the constraint boundary.

**Definition 1.** For above constrained optimization problem (COP), we define the function:  $\phi(x) : D \rightarrow R$  and let  $S = \{\vec{q} \mid \vec{q} \in D \wedge f_i^k \leq 0 \wedge f_i^{nt+k} \leq 0\}$

$$\phi(\vec{q}) = \sum_{k=1}^{n_t} \sum_{i=1}^{n_r} (G_i^k + G_i^{n_t+k}),$$

where

$$(33) \quad G_i^k(\vec{q}) = \begin{cases} 1/2, & f_i^k(\vec{q}) \leq 0, \\ 1/(1 + \exp(f_i^k(\vec{q}))), & \text{otherwise,} \end{cases}$$

$$(34) \quad G_i^{n_t+k}(\vec{q}) = \begin{cases} 1/2, & f_i^{n_t+k}(\vec{q}) \leq 0, \\ 1/(1 + \exp(f_i^{n_t+k}(\vec{q}))), & \text{otherwise.} \end{cases}$$

It is obvious that  $\phi(\vec{q}) = n_r \cdot n_t$  when  $\vec{q} \in S$ ,  $0 < \phi(\vec{q}) < n_r \cdot n_t$  when  $\vec{q} \notin S$ , and the more of the number that  $\vec{q}$  obeys the constrained conditions, the less of the value of  $\phi(\vec{q})$ .

**Definition 2.** Suppose that  $\vec{q}$  and  $\vec{p}$  are two different individuals from the next two generations, we define the following function:

$$(35) \quad \text{prior}(\vec{q}, \vec{p}) = \begin{cases} 1, & \phi(\vec{q}) = \phi(\vec{p}) \wedge J_h(\vec{q}) < J_h(\vec{p}) \vee \phi(\vec{q}) > \phi(\vec{p}), \\ 0, & \text{otherwise.} \end{cases}$$

If  $\text{prior}(\vec{q}, \vec{p}) = 1$ , it means that  $\vec{q}$  is prior to  $\vec{p}$ .

Then, we give the brief outline of constrained algorithm:

**Step 1.** Set the control parameter: the number of the population  $N_p$ , mutation operator  $F$ , crossover rate  $CR$ , the most generation  $G_{max}$  and the stop criteria.

**Step 2.** Initialize population. Set  $G = 0$ , and define  $N_p$   $n_s$ -dimensional vectors, so-called individuals, which encode the candidate solutions:  $\vec{q}_{i,G} = (q_{i,G}^1, \dots, q_{i,G}^{n_s})$ ,  $i = 1, 2, \dots, N_p$  towards the global optimum. The initial population should better cover the entire search space as much as possible by uniformly randomizing individuals within the search space constrained by the prescribed minimum and maximum parameter bounds  $\vec{q}^{min} = (q_1^{min}, \dots, q_{n_s}^{min})$  and  $\vec{q}^{max} = (q_1^{max}, \dots, q_{n_s}^{max})$ . For example, the initial value of the  $j$ th parameter in the  $i$ th individual at the generation  $G$  is generated by:

$$q_{i,G}^j = q_j^{min} + \text{rand}(0, 1) \cdot (q_j^{max} - q_j^{min}),$$

where  $\text{rand}(0, 1)$  is a random number in  $[0, 1]$ .

**Step 3.** Mutation operation. For each vector  $\vec{q}_{i,G}$ ,  $i = 1, 2, \dots, N_p$ , a perturbed vector  $\vec{v}_{i,G+1}$ , called mutant vector, is generated according:

$$\vec{v}_{i,G+1} = \vec{q}_{r_1,G} + F \cdot (\vec{q}_{r_2,G} - \vec{q}_{r_3,G}),$$

where  $r_1, r_2, r_3 \in [1, N_p]$  are integers, they are chosen randomly different from each other and different from index  $i$ .  $F \in [0, 2]$  is a real and constant factor, which control the amplification of the difference variation  $(\vec{q}_{r_2,G} - \vec{q}_{r_3,G})$ .

*Remark 3.2.1* It should be noted that there are also other perturbed methods. We list the following four methods frequently used mutation strategies implemented in the code.

$$(36) \quad \begin{aligned} \vec{v}_{i,G+1} &= \vec{q}_{best,G} + F \cdot (\vec{q}_{r_1,G} - \vec{q}_{r_2,G}), \\ \vec{v}_{i,G+1} &= \vec{q}_{i,G} + F \cdot (\vec{q}_{best,G} - \vec{q}_{i,G}) + F \cdot (\vec{q}_{r_1,G} - \vec{q}_{r_2,G}), \\ \vec{v}_{i,G+1} &= \vec{q}_{best,G} + F \cdot (\vec{q}_{r_1,G} - \vec{q}_{r_2,G}) + F \cdot (\vec{q}_{r_3,G} - \vec{q}_{r_4,G}), \\ \vec{v}_{i,G+1} &= \vec{q}_{r_1,G} + F \cdot (\vec{q}_{r_2,G} - \vec{q}_{r_3,G}) + F \cdot (\vec{q}_{r_4,G} - \vec{q}_{r_5,G}). \end{aligned}$$

**Step 4.** Crossover operation. Crossover operation is applied to each pair of target vector  $\vec{q}_{i,G}$  and its corresponding mutant vector  $\vec{v}_{i,G+1}$  to generate a trial

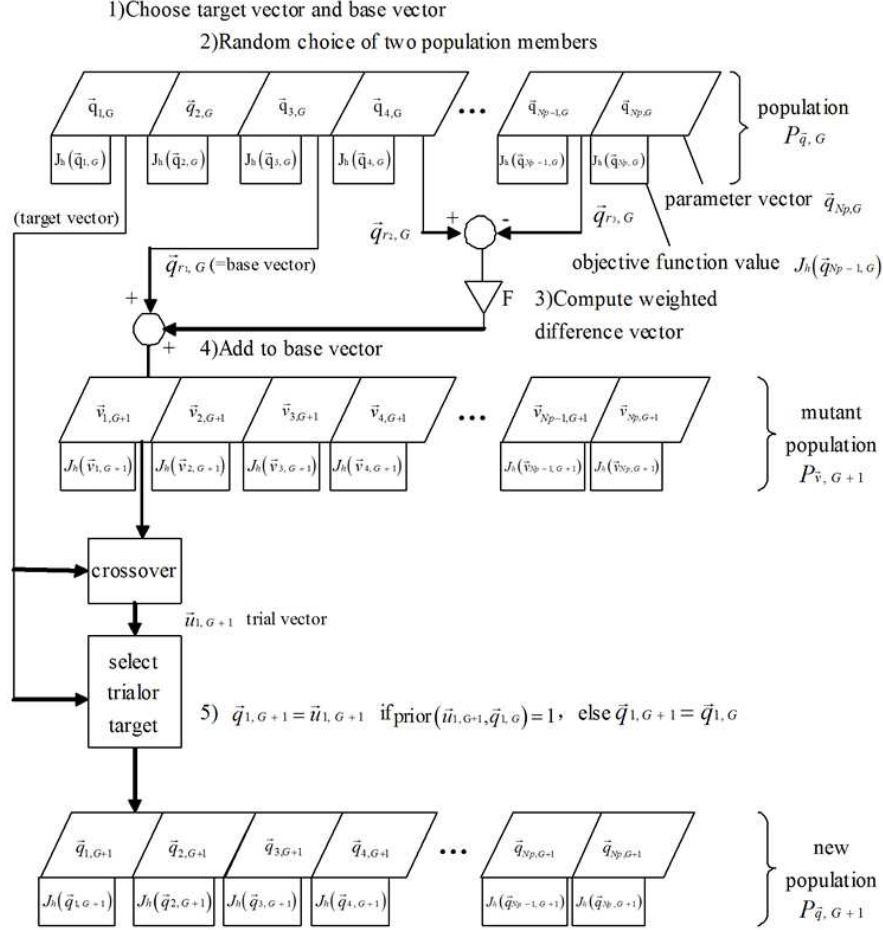


**Fig. 2.** Schematic representation of the Differential Evolution (DE) algorithm.

vector:  $\vec{u}_{i,G+1} = (u_{i,G+1}^1, \dots, u_{i,G+1}^{n_s})$ . In the basic version, DE employs the binomial crossover defined as below:

$$(37) \quad u_{i,G+1}^j = \begin{cases} v_{i,G+1}^j, & \text{if } \text{randb}(j) \leq CR \text{ or } j = \text{rnbr}(i), \\ \vec{q}_{i,G}^j, & \text{otherwise,} \end{cases}$$

where  $j = 1, 2, \dots, n_s$ ,  $\text{randb}$  is a list of random number and  $\text{randb}(j)$  is the  $j$ th number,  $\text{rnbr}$  is a randomly chosen integer in  $[1, n_s]$ , the crossover rate  $CR$  is a user-specified constant within the range  $[0, 1]$ .

*Remark 3.2.2* There exists another exponential crossover operator in addition to binomial crossover.

**Step 5.** Selection operation. After the mutation and crossover operations, the trial vector  $\vec{u}_{i,G+1}$  is compared to the old vector  $\vec{q}_{i,G}$ . If the trial vector has an equal or better objective value, then it replaces the old vector in the next generation. This can be presented as follows:

$$(38) \quad \vec{q}_{i,G+1} = \begin{cases} \vec{u}_{i,G+1}, & \text{if } \text{prior}(\vec{u}_{i,G+1}, \vec{q}_{i,G}) = 1, \\ \vec{q}_{i,G}, & \text{otherwise.} \end{cases}$$

**Step 6.** Let  $G = G + 1$ . If  $G \leq G_{max}$  and the stop criteria is not satisfied, turn to Step 2. Otherwise, output the optimal solution  $\vec{q}_{i,G+1}$ .

**4. Numerical experiments**

**4.1 Numerical tests for solving pollution problem.** In this sub-section, we will first give examples to show the error and ratio of the improved upwind finite volume scheme (IUFVS) for solving the pollution problems.

**Example 1.** In the first example, we consider a problem with the right side function as

$$\begin{aligned}
 f(x, y, t) = & \exp(t)x(x-1)^2y^2(y-1)^2 \\
 & + \exp(t)y^2(y-1)^2[-D_x(6x-4) + v_x(3x^2-4x+1)] \\
 & + \exp(t)x(x-1)^2[-D_y(12y^2-12y+2) + v_y(4y^3-6y^2+2y)],
 \end{aligned}$$

the initial value is  $u_0(x, y) = x(x-1)^2y^2(y-1)^2$ . In this case, the exact solution is  $u(x, y, t) = \exp(t)x(x-1)^2y^2(y-1)^2$ .

In numerical computation, the domain is  $\Omega = [0, 1] \times [0, 1]$ , the spatial step sizes are taken as  $h_x = 1/N$  and  $h_y = 1/N$ , and the final time is  $T = 1$ . The errors and the error orders in  $L^2$ -norm are given in Table 1, where  $N = 10, 20, 40, 80$  and  $\Delta t = 10^{-4}$ . From Table 1, we can see clearly that our IUFVS is second order in the spatial step size.

TABLE 1. Errors and Ratios of the IUFVS for Example 1 with  $v_x = 0.1, v_y = 0$ , and  $D_x = D_y = 10^{-l}, l = 1, 2, 3$ , and  $T = 1$ .

N	$D_x = D_y = 10^{-3}$		$D_x = D_y = 10^{-2}$		$D_x = D_y = 10^{-1}$	
	$L^2$ -error	Ratio	$L^2$ -error	Ratio	$L^2$ -error	Ratio
10	5.0718(10 <sup>-4</sup> )		2.4970(10 <sup>-4</sup> )		5.2545(10 <sup>-4</sup> )	
20	2.2271(10 <sup>-4</sup> )	1.1873	6.7738(10 <sup>-5</sup> )	1.8821	1.1846(10 <sup>-4</sup> )	2.1492
40	8.7516(10 <sup>-5</sup> )	1.3476	1.7620(10 <sup>-5</sup> )	1.9427	2.7593(10 <sup>-5</sup> )	2.1020
80	3.0262(10 <sup>-5</sup> )	1.5320	4.3701(10 <sup>-6</sup> )	2.0115	6.4180(10 <sup>-6</sup> )	2.1041

**Example 2.** We consider the pollution problem with the dispersion coefficients  $D_x = D_y = 0.1$ , and velocity components  $v_x = 0.5$  and  $v_y = 0$ , and the reaction coefficient  $R = 0.01$ . Suppose every outfall has the same discharge flux  $q_l = 5.0, l = 1, 2, \dots, n_s$ . The domain is  $\Omega = [0, 1] \times [0, 1]$ . The space step sizes are  $h_x = h_y = 0.01$  and the time step size is  $\Delta t = 10^{-2}$ . The concentration distribution of pollution in the whole domain at different time are shown in Figures 3 - 5.

Further, Figure 6 shows the comparisons of the pollutant concentrations on the line of  $y = 0.5$  with different space step sizes and for the same discharge rates of outfalls  $q_l = 5.0, l = 1, 2, \dots, n_s$ . From these figures, we can see that the IUFVS is convergent when the step size decreases.

**4.2 Numerical experiments for the optimal control problems**

In this subsection, we will present numerical experiments to show the performance of the proposed optimal control approach. While the first experiment shows the numerical results for the objective problem of only the weighted deviation between simulation concentration and the allowable environmental concentration, the

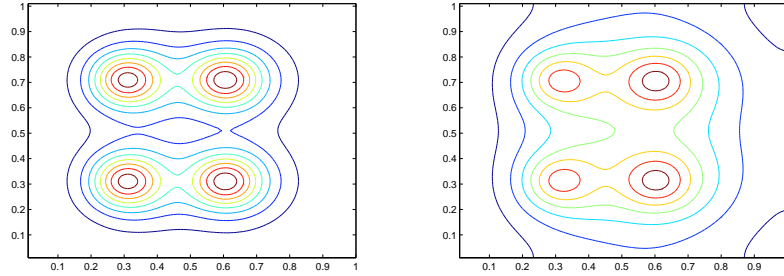


**Fig. 3.** Concentration distributions at  $T = 0.1$  (left) and at  $T = 0.3$  (right).

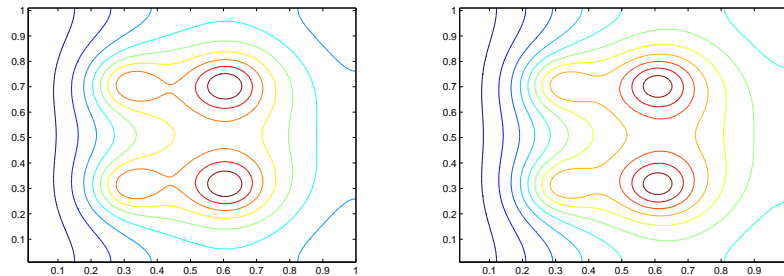


**Fig. 4.** Concentration distributions at  $T = 0.5$  (left) and at  $T = 0.7$  (right).

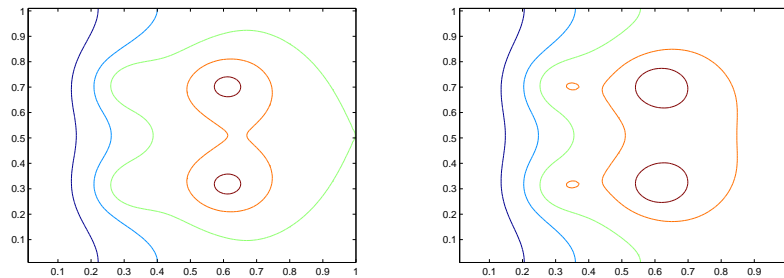


**Fig. 5.** Concentration distributions at  $T = 0.9$  (left) and at  $T = 1.1$  (right).

following two experiments will consider the global optimal control problems of minimizing both the concentration differences and the emission reduction cost.

**Simulation 1.** In this simulation, we consider the optimal control problem of minimizing the concentration differences. The observation concentrations are taken from the concentrations obtained by perturbing the numerical concentrations, which are evaluated from an actual smallest disposal flux, as defined by

$$(39) \quad C_s^{*k} = C_s^k + \xi C_s^k (2rand(\cdot) - 1),$$

for  $s = 1, 2, \dots, n_r$ .

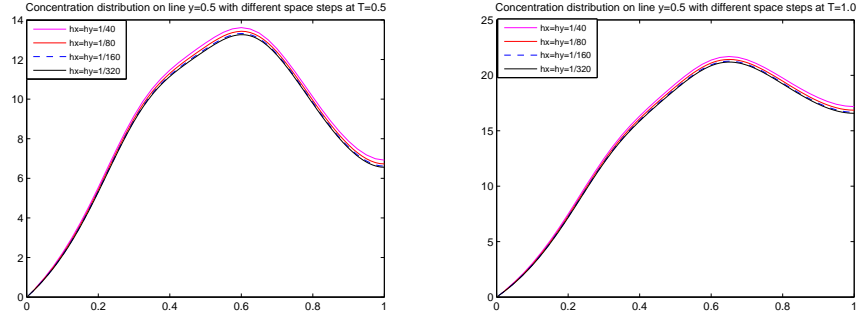


**Fig. 6.** Concentration distributions on line  $y = 0.5$  with different space steps at  $T = 0.5$  (left) and at  $T = 1.0$  (right).

Perturbing the numerically simulated concentrations is analogous to collecting and then testing multiple samples of pollutant at spatiotemporal observation locations. It is assumed that observation datum obey a normal distribution. The mean of the normal distribution is the exact datum  $C_s^k$ , which can be computed from the simulation with actual smallest fluxes. The standard deviations equal to some fraction  $\xi$  of the exact datum, called noise levels. While  $\xi = 0$  means that it is error free. The  $rand(\cdot)$  is a random number between  $(0, 1)$ . We can use this way to identify the disposal flux on the condition that knowing the observation data in advance.

We consider that the pollution flow occurs in a rectangle domain  $\Omega = [0, 2] \times [0, 1]$  during a period of  $T = 1.0$ . The diffusion coefficients are  $D_x = D_y = 0.1$ . The velocity components are  $v_x = 0.5$  in the direction of  $x$ -direction and  $v_y = 0$  in the  $y$ -direction. The self-purifying coefficient is  $R = 0.01$ . Besides, the initial value is taken as  $c_0(x, y) = 0$ .

**Case 1.1**

Assuming that there are four pollution sources and four observation points, located symmetrically in the domain. The pollution source locations are set as  $S_1 = (0.7, 0.3)$ ,  $S_2 = (1.3, 0.3)$ ,  $S_3 = (1.3, 0.6)$ ,  $S_4 = (0.7, 0.6)$  and the observation points are located at  $O_1 = (0.4, 0.2)$ ,  $O_2 = (1.6, 0.2)$ ,  $O_3 = (1.6, 0.7)$ , and  $O_4 = (0.4, 0.7)$ . Performance evaluations are done for error free and with noise level of  $\xi = 0.005$  and  $\xi = 0.01$  in observation data. The numerical results of solving the optimal control problem are presented in Tables 2-3. In Table 2, the space step sizes are  $\Delta x = 0.05$  and  $\Delta y = 0.05$ , the time step size is  $\Delta t = 0.05$ , while in Table 3, the step sizes are taken smaller as  $\Delta x = \Delta y = 0.025$  and  $\Delta t = 0.025$ .

TABLE 2. Numerical simulation results of the optimal control problems with sources at  $S_l, l = 1, 2, 3, 4$  by  $\Delta x = \Delta y = 0.05$  and  $\Delta t = 0.05$ .

	actual flux	$\xi = 0$	$\xi = 0.005$		$\xi = 0.01$	
		simul. flux	simul. flux	err ( $10^{-4}$ )	simul. flux	err ( $10^{-3}$ )
$S_1$	2.1	2.1000	2.1004	2.119	2.0915	4.058
$S_2$	4.1	4.1000	4.0967	7.949	4.0958	1.011
$S_3$	6.1	6.1000	6.0975	4.123	6.0758	3.975
$S_4$	8.1	8.0999	8.0978	2.663	8.1119	1.471

TABLE 3. Numerical simulation results of the optimal control problem with sources at  $S_l, l = 1, 2, 3, 4$  by  $\Delta x = \Delta y = 0.025$  and  $\Delta t = 0.025$ .

	actual flux	$\xi = 0$	$\xi = 0.005$		$\xi = 0.01$	
		simul. flux	simul. flux	err ( $10^{-4}$ )	simul. flux	err ( $10^{-3}$ )
$S_1$	2.1	2.1000	2.1003	1.481	2.1024	1.149
$S_2$	4.1	4.0999	4.1009	2.312	4.1049	1.192
$S_3$	6.1	6.1000	6.1015	2.502	6.0983	0.276
$S_4$	8.1	8.1000	8.0988	1.507	8.0976	0.299

From Tables 2 - 3, we can see that the numerical optimized fluxes are in great agreement with actual values. When some bigger noises are used in observed data the optimized fluxes are of error. Comparing the errors of the computed fluxes with different space and time steps, the errors are smaller when the step sizes are small. This indicates that the optimal control simulation results are better if the schemes have higher accuracy.

**Case 1.2**

In this case, we consider that the four pollution sources are asymmetrically located in the domain. The locations of pollution sources are at  $S_1 = (0.7, 0.3)$ ,  $S'_2 = (1.3, 0.4)$ ,  $S'_3 = (1.3, 0.7)$ , and  $S'_4 = (0.8, 0.6)$ , while the observation locations are at the same points as Case 1.1. Tables 4 - 5 give the numerical results and relative errors by using different noise levels in observed measurement data, where the actual disposal fluxes are polluted differently. The space step sizes are used as  $\Delta x = 0.025$  and  $\Delta y = 0.025$  and the time step size is used as  $\Delta t = 0.025$ .

TABLE 4. Numerical simulation results of the optimal control problem with sources at  $S_1, S'_l, l = 2, 3, 4$  by  $\Delta x = \Delta y = 0.025$  and  $\Delta t = 0.025$ .

	actual flux	$\xi = 0$	$\xi = 0.005$		$\xi = 0.01$	
		simul. flux	simul. flux	err ( $10^{-4}$ )	simul. flux	err ( $10^{-3}$ )
$S_1$	2.1	2.1000	2.0983	8.295	2.0972	1.314
$S'_2$	4.1	4.1000	4.0986	3.410	4.0998	0.032
$S'_3$	6.1	6.0999	6.1008	0.128	6.1027	0.450
$S'_4$	8.1	8.1000	8.0955	5.591	8.0996	0.045

TABLE 5. Numerical simulation results of the optimal control problem with sources at  $S_1, S'_l, l = 2, 3, 4$  by  $\Delta x = \Delta y = 0.025$  and  $\Delta t = 0.025$ .

	actual flux	$\xi = 0$	$\xi = 0.005$		$\xi = 0.01$	
		simul. flux	simul. flux	err ( $10^{-4}$ )	simul. flux	err ( $10^{-3}$ )
$S_1$	22	22.0000	22.0000	0.001	22.0468	2.127
$S'_2$	24	24.0000	24.0115	4.783	24.0227	0.947
$S'_3$	26	26.0000	25.9950	1.935	26.0173	0.664
$S'_4$	28	28.0000	28.0030	1.057	27.9234	2.734

The results in Tables 4 - 5 for Case 1.2 are consistent with results for Case 1.1. They show that no matter how much the values of the actual fluxes are, the optimal identified disposal fluxes have small errors if the random measurements are at small error levels.

**Simulation 2.** Now, we consider the global optimal control problems of minimizing both the weighted concentration differences between the simulated concentrations and the allowable smallest environmental concentrations and the emission reduction cost.

The domain is  $\Omega = [0, 5] \times [0, 1]$  and the time period is  $T = 1.0$ . The diffusion coefficients are  $D_x = 0.1$  and  $D_y = 0.1$ , the velocity is  $v_x = 1.0$ , and  $v_y = 0$ , and the self-purifying coefficient is  $R = 0.001$ . The initial value is  $c_0(x, y) = 0$ . In computation, we take  $\Delta x = 0.025$ ,  $\Delta y = 0.025$ , and  $\Delta t = 0.025$ . There are four pollution sources in the domain. There are four small domains that need be protected, where the pollution concentrations are restricted in a certain extent. In the case, we consider the special areas as some points, which are the observation location points. Further, the lower bound of the disposal fluxes is the minimal emission amount and the upper bound of disposal flux can refer to the situation that the worst pollution achieves.

We use  $C_s^*$ ,  $s = 1, 2, \dots, n_r$ , to be the concentrations that obtained when the disposal fluxes are the lower bounds and with a noise  $\xi = 0.01$ . In the view of the global optimal control, we will aim at determining the disposal fluxes that minimum the deviations between  $C_s^*$  and the computed concentrations and ensuring the emission reduction cost as smaller as possible, where the cost part of the objective function is as

$$(40) \quad g_l(q_l) = c_1(l)Q_l^2 + c_2(l)Q_l, \quad l = 1, 2, \dots, n_s,$$

and  $Q_l = \frac{q_{max} - q_l}{q_{max}}$  is called the emission reduction rate at source  $S_l$ , and  $c_1(l)$  and  $c_2(l)$  are parameters.

**Case 2.1**

We consider that the four pollution sources are symmetrically located in the domain and the observation sites are located around the pollution sources, where the sources are at  $S_1 = (2.0, 0.3)$ ,  $S_2 = (3.0, 0.3)$ ,  $S_3 = (3.0, 0.7)$ ,  $S_4 = (2.0, 0.7)$  and the observations are at  $O_1 = (1.0, 0.2)$ ,  $O_2 = (4.0, 0.2)$ ,  $O_3 = (4.0, 0.8)$ , and  $O_4 = (1.0, 0.8)$ . The lower and upper bounds of the disposal fluxes are  $\vec{q}_{min} = (6.0, 5.0, 5.0, 6.0)^\tau$  and  $\vec{q}_{max} = (20.0, 20.0, 20.0, 20.0)^\tau$ .

TABLE 6. Numerical results of the disposal fluxes with different cost functions at sources  $S_l, l = 1, 2, 3, 4$ , and the observation locations at  $O_s, s = 1, 2, 3, 4$ .

	fluxes without cost	same cost function		different cost functions	
		fluxes	reduction rate	fluxes	reduction rate
$S_1$	6.0000	11.3721	43.14%	10.5782	47.11%
$S_2$	5.0218	5.9963	70.02%	5.7380	71.31%
$S_3$	5.0008	5.9504	70.25%	5.5334	72.33%
$S_4$	6.0000	11.1525	44.24%	16.3900	18.05%

The numerical results are presented in Table 6. For the case of one same cost function at four source points, the coefficients are  $c_1(l) = 26.0, l = 1, 2, 3, 4$ , and

$c_2(l) = 15.0, l = 1, 2, 3, 4$ , while for the case of the different cost functions at four source points, the coefficients are  $c_1(1) = 32.0, c_2(1) = 15.0, c_1(2) = 25.0, c_2(2) = 12.0, c_1(3) = 15.0, c_2(3) = 9.0$ , and  $c_1(4) = 47.0, c_2(4) = 38.0$ , respectively.

**Case 2.2**

In this case, we show the affection of the observation locations over affections of reduction rates at pollution sources. The lower and upper bounds of the disposal fluxes at source points are  $\vec{q}_{min} = (8.0, 5.0, 5.0, 8.0)^T$  and  $\vec{q}_{max} = (30.0, 30.0, 30.0, 30.0)^T$ . According to the observation positions, where they are in the upstream or downstream, the four situations for the observation zones are different from the situation in Case 2.1.

In Table 7, the observation sites are all in the upstream of the pollution sources, they are  $O_1 = (1.0, 0.2), O_2 = (1.5, 0.2), O_3 = (1.5, 0.8)$ , and  $O_4 = (1.0, 0.8)$ . In Table 8, two sites are located in upstream, and the other two located between the pollution sources, they are  $O_1 = (1.0, 0.2), O_2^* = (2.5, 0.2), O_3^* = (2.5, 0.8), O_4 = (1.0, 0.8)$ . In Table 9, all the four observation sites are in the downstream, they are  $O_1' = (3.5, 0.2), O_2 = (4.0, 0.2), O_3 = (4.0, 0.8)$ , and  $O_4' = (3.5, 0.8)$ . In Table 10, two sites are located in downstream, and the other two located among the pollution sources, they are  $O_1^* = (2.5, 0.2), O_2 = (4.0, 0.2), O_3 = (4.0, 0.8)$ , and  $O_4^* = (2.5, 0.8)$ .

TABLE 7. Numerical results of the disposal fluxes with different cost functions at sources  $S_l, l = 1, 2, 3, 4$ , with observations at  $O_s, s = 1, 4$  and  $O'_s, s = 2, 3$ .

	fluxes without cost	same cost function		different cost functions	
		fluxes	reduction rate	fluxes	reduction rate
$S_1$	8.0006	8.7555	70.82%	8.4276	71.91%
$S_2$	5.0000	30.000	0%	30.000	0%
$S_3$	5.0000	30.000	0%	30.000	0%
$S_4$	8.0110	8.7695	70.77%	9.8059	67.31%

From Table 7, we can see that the disposal fluxes are almost the minimum fluxes when doesn't consider the reduction cost optimization. For the two pollution sources in the downstream, the disposal fluxes contain the upper bounds unchanged whether in situation for different cost functions or same function. In the situation of same cost function, the first emission rate is close to the fourth one, which means that the two pollutants in the upstream should reduce almost the same amount of emission when the unit price is the same. While for different cost function, the fourth pollutant has a higher cost function coefficients, its emission reduction rate is smaller than the first one.

The disposal fluxes in Table 8 are still almost the minimum fluxes when doesn't consider the reduction cost optimization in this case. With considering the reduction cost term, there are two pollutants, which located in the downstream, almost does not need reduce the emission. While the emission reduction rates are same with same cost function, it is smaller when the cost is bigger.

Comparing this case in Table 8 with the previous one in Table 7, the simulation results have the same trends. It can be concluded that the pollutants in the

TABLE 8. Numerical results of the disposal fluxes with different cost functions at sources  $S_l, l = 1, 2, 3, 4$  and with observations at  $O_s, s = 1, 4$  and  $O_s^*, s = 2, 3$ .

	fluxes without cost	same cost function		different cost functions	
		fluxes	reduction rate	fluxes	reduction rate
$S_1$	8.00000	8.5373	71.542%	8.3609	72.13%
$S_2$	5.00001	30.000	0%	30.000	0%
$S_3$	5.00005	30.000	0%	29.999	0.003%
$S_4$	8.01367	8.5369	71.543%	8.5808	71.40%

downstream almost don't need to reduce the emission, while the pollutants in the upstream need reduce so much to tend to the lower bounds.

TABLE 9. Numerical results of the disposal fluxes with different cost functions at sources  $S_l, l = 1, 2, 3, 4$  and with observations at  $O'_s, s = 1, 4$  and  $O_s, s = 2, 3$ .

	fluxes without cost	same cost function		different cost functions	
		fluxes	reduction rate	fluxes	reduction rate
$S_1$	8.0133	29.8273	0.58%	16.2644	45.79%
$S_2$	5.0002	5.3831	82.06%	5.0000	83.33%
$S_3$	5.0055	5.3246	82.25%	5.0000	83.33%
$S_4$	8.0003	22.5125	24.96%	29.3126	2.29%

For this situation, the observation site are all in the downstream compared to the pollution sources. From Table 9, we can see that the disposal fluxes are almost the minimum fluxes without considering the cost optimization. For the second and third pollution sources, which located close to the observation site, the disposal fluxes reduced to the lower bounds when adopting different cost function, or close to the lower bounds when with the same cost function. That is to say, the pollution sources close to the protected zones should make more contribute to reduce the pollutant.

TABLE 10. Numerical results of the disposal fluxes with different cost functions at sources  $S_l, l = 1, 2, 3, 4$  and with observations at  $O_s^*, s = 1, 4$  and  $O_s, s = 2, 3$ .

	fluxes without cost	same cost function		different cost functions	
		fluxes	reduction rate	fluxes	reduction rate
$S_1$	8.0002	8.7188	70.94%	8.0000	73.33%
$S_2$	5.0000	5.2035	82.66%	5.9651	80.12%
$S_3$	5.0006	5.8181	80.61%	5.1954	82.68%
$S_4$	8.0070	9.2581	69.14%	10.4364	65.21%

From Table 10, no matter the cost functions are different or same, the plants should reduce the emission nearly to the lower bounds, this is suitable for the situation that every protected zone is located in the downstream of each pollution

sources. In the column of fluxes with different cost functions, comparing the first with the fourth, the fourth that has higher price per unite reduces less than the first. Similar conclusion is held for the second and third.

**Case 2.3**

We numerically observe the effects of flow velocities to the optimal control results. Numerical results are presented in Table 11 where the flow velocity is  $v_x = 2.0$  and  $v_y = 0.0$  and in Table 12 where the velocity is  $v_x = 0.5$  and  $v_y = 0.0$ .

TABLE 11. Numerical simulation results of the disposal fluxes with different cost functions at sources  $S_l, l = 1, 2, 3, 4$  and with velocity  $v_x = 2.0$  and  $v_y = 0.0$ .

	fluxes without cost	same cost function		different cost functions	
		fluxes	reduction rate	fluxes	reduction rate
$S_1$	6.0000	16.7060	16.47%	12.9393	35.30%
$S_2$	5.0000	5.0000	75.00%	5.0000	75.00%
$S_3$	5.0097	5.0000	75.00%	5.0000	75.00%
$S_4$	6.0000	15.5710	22.15%	19.5625	2.19%

TABLE 12. Numerical results of the disposal fluxes with different cost functions at sources  $S_l, l = 1, 2, 3, 4$  and with velocity of  $v_x = 0.5$  and  $v_y = 0.0$ .

	fluxes without cost	same cost function		different cost functions	
		fluxes	reduction rate	fluxes	reduction rate
$S_1$	6.0000	7.4293	62.85%	6.5568	66.67%
$S_2$	5.0000	5.8906	70.55%	5.3181	68.41%
$S_3$	5.0065	5.9014	70.49%	5.2587	73.71%
$S_4$	6.0108	7.4433	62.78%	9.5326	52.34%

From Tables 11 - 12 and Table 6, we can see that a smaller emission reduction rate in the upstream can be made when the flow has a bigger velocity, while a bigger reduction rate in the downstream can be applied. Further, the disposal fluxes in the downstream can be reduced to the minimum value if the flow velocity is big enough.

**Simulation 3.** In this simulation, we consider the exponential cost function like (11). That is because the unit cost of emission reduction of some pollutants are huge, it vary as the form of exponents. For others' small variation of cost, we still use polynomial cost function (10).

The domain is still  $\Omega = [0, 5] \times [0, 1]$  and  $T = 1.0$ . The numerical results of discharge fluxes obtained by solving the optimal control model are displayed in Table 13. The lower and upper bounds of the disposal fluxes are  $\vec{q}_{min} = (6.0, 5.0, 5.0, 6.0)^T$  and  $\vec{q}_{max} = (26.0, 25.0, 25.0, 26.0)^T$ . The first and the fourth pollution source points adopt the polynomial function as the cost of emission reduction, while the second and the third proposal the exponential function, they are:

$$(41) \quad g_l(q_l) = c_1(l)(e^{c_2(l)Q_l} - 1), \quad l = 2, 3.$$

The coefficients of the same cost function are  $c_1(1) = c_1(4) = 26.0$ ,  $c_2(1) = c_2(4) = 15.0$  and  $c_1(2) = c_1(3) = 15.0$ ,  $c_2(2) = c_2(3) = 8.0$ . The coefficients of the different cost functions are  $c_1(1) = 46.0$ ,  $c_2(1) = 23.0$ ,  $c_1(2) = 21.0$ ,  $c_2(2) = 14.0$ ,  $c_1(3) = 15.0$ ,  $c_2(3) = 8.0$ , and  $c_1(4) = 26.0$ ,  $c_2(4) = 15.0$ .

TABLE 13. Numerical simulation results of disposal fluxes with joint polynomial and exponential cost functions at sources  $S_l, l = 1, 2, 3, 4$  and with observations at  $O_s, s = 1, 2, 3, 4$ .

	fluxes without cost	same cost function		different cost functions	
		fluxes	reduction rate	fluxes	reduction rate
$S_1$	6.0080	11.0867	57.36%	12.2442	52.91%
$S_2$	5.0000	15.7917	36.83%	20.9011	16.39%
$S_3$	5.0071	16.7075	33.17%	14.9261	40.29%
$S_4$	6.0135	11.0537	57.49%	10.6517	59.03%

From Table 13, the emission reduction rates are nearly identical for same cost function, while those pollution sources have a small reduction rate because the cost of reducing one unit pollutant is big. But the important point is that the pollutants that adopt exponential cost functions require much smaller emission reduction rate than those with polynomial cost functions.

### Acknowledgments

This research was supported by the Natural Sciences and Engineering Research Council of Canada and by the National Natural Science Foundation of China under grant 11271232.

### References

- [1] S. Alapati, Z. J. Kabala, Recovering the release history of a groundwater contaminant using a non-linear least-squares method, *Hydrol. Process.*, 14 (2000), 1003-1016.
- [2] I. Butera, M. G. Tanda, A geostatistical approach to recover the release history of groundwater pollutants, *Water Resour. Res.*, 39(12) (2003), 1372, doi:10.1029/2003WR002314.
- [3] S. Das, P. N. Suganthan, Differential Evolution: A survey of the state-of-the-Art, *IEEE Transaction on Evolutionary Computation*, 15(1) (2011), 4-31.
- [4] C. Du, D. Liang, An efficient S-DDM iterative approach for compressible contamination fluid flows in porous media, *J. Comput. Phys.*, 229 (2010), 4501-4521.
- [5] K. Fu, D. Liang, W. Wang, M. Cui, The time second-order characteristic FEM for nonlinear multicomponent aerosol dynamic equations in environment, *Int. J. Numer. Anal. Modelling*, 12 (2015), 211 - 229.
- [6] P. S. Huyakorn, K. Nukula, Solution of transient transport equation using an upstream finite element scheme, *Appl. Math. Model*, 3 (1979), 7-17.
- [7] R. D. Lazarrov, I. D. Mishev, P. S. Vassilevski, Finite volume methods for convection-diffusion problems, *SIAM J. Numer. Anal.*, 33 (1996), 31-55.
- [8] D. Liang, W. D. Zhao, An optimal weighted upwind covolume method on non-standard grids for convection-diffusion problems in 2D, *Int. J. Numer. Methods Eng.*, 67 (2006), 553-577
- [9] S. Kukkonen, J. Lampinen, Constrained real-parameter optimization with generalized Differential Evolution, *IEEE Congress on Evolutionary Computation*, (2006), 207-214.
- [10] P. S. Mahar, B. Datta, Optimal identification of ground-water pollution source and parameter estimation, *J. Water Resour. Plan. Mandge.*, 127(1) (2001), 20-29.
- [11] S. Sharma, G. P. Rangaiah, An improved multi-objective differential evolution with a termination criterion for optimizing chemical processes, *Comput. Chem. Eng.*, 56 (2013), 155-173.
- [12] R. M. Singh, B. Datta, Identification of groundwater pollution sources using GA-based linked simulation optimization model, *J. Hydrol. Eng.*, 11(2) (2006), 101-109.

- [13] R. Storn, K. V. Price, Differential evolution: A simple and efficient adaptive scheme for global optimization over continuous spaces, ICSI, USA, Tech. Rep. TR-95-012 (1995), <http://icsi.berkeley.edu/storn/litera.html>
- [14] R. Storn, System design by constraint adaptation and differential evolution, *IEEE Trans. Evol. Comp.*, 3(1) (1999), 22-34.
- [15] A. Y. Sun, S. L. Painter, G. W. Wittmeyer, A constrained robust least squares approach for contaminant release history identification, *Water Resour. Res.*, 42 (2006), W04414, doi:10.1029/2005ER004312.
- [16] P. Tamamidis, A new upwind scheme on triangular meshes using the finite volume method, *Comput. Methods Appl. Mech. Engrg.*, 124 (1995), 15-31.
- [17] D. X. Zou, H. K. Liu, L. Q. Gao, S. LI, A novel modified differential evolution algorithm for constrained optimization problems, *Comput. Math. Appl.*, 61 (2011), 1608-1623.

School of Mathematics, Shandong University, Jinan, Shandong, 250100, China  
*E-mail:* [yuanyujing88@163.com](mailto:yuanyujing88@163.com)

Department of Mathematics and Statistics, York University, Toronto, Ontario, M3J 1P3, Canada  
*E-mail:* [dliang@mathstat.yorku.ca](mailto:dliang@mathstat.yorku.ca)